Applied Catalysis B: Environmental 269 (2020) 118769

Contents lists available at ScienceDirect

Applied Catalysis B: Environmental

journal homepage: www.elsevier.com/locate/apcatb

Elucidating the promotional effect of a covalent triazine framework in aerobic oxidation

Sara Abednatanzi[a], Parviz Gohari Derakhshandeh[a], Pieter Tack[b], Francesco Muniz-Miranda[c], Ying-Ya Liu[d], Jonas Everaert[e], Maria Meledina[f,g], Flore Vanden Bussche[a,e], Laszlo Vincze[b], Christian V. Stevens[e], Veronique Van Speybroeck[c], Henk Vrielinck[h], Freddy Callens[h], Karen Leus[a], Pascal Van Der Voort[a,*]

[a] Center for Ordered Materials, Organometallics and Catalysis (COMOC), Department of Chemistry, Ghent University, Krijgslaan 281-S3-B-9000, Ghent, Belgium
[b] X-ray Microspectroscopy and Imaging (XMI), Department of Chemistry, Ghent University, Krijgslaan 281 (S12), 9000, Ghent, Belgium
[c] Center for Molecular Modeling (CMM), Ghent University, Technologiepark 903, B-9052, Zwijnaarde, Belgium
[d] State Key Laboratory of Fine Chemicals, Dalian University of Technology, 116024, Dalian, PR China
[e] Department of Green Chemistry and Technology, Faculty of Bioscience Engineering, Ghent University, Coupure Links 653, 9000, Ghent, Belgium
[f] RWTH Aachen University, Central Facility for Electron Microscopy, D-52074, Aachen, Germany
[g] Forschungszentrum Jülich GmbH, Ernst Ruska-Centre (ER-C 2), D-52425, Jülich, Germany
[h] Department of Solid State Sciences, Ghent University, Krijgslaan 281-S1, B-9000, Ghent, Belgium

ARTICLE INFO

Keywords:
Covalent triazine frameworks
Heterogeneous catalysis
Synergistic effect
Oxygen activation
Mechanistic studies

ABSTRACT

Synergistic catalysis holds great promise to enhance the catalytic performance of heterogeneous catalysts suffering from sluggish reaction kinetics. Much effort has been dedicated to the development of bimetallic systems in which the two promoter elements display synergistic benefits compared to monometallic counterparts. However, the use of bimetallic catalysts inescapably raises the cost of preparation and environmental issues. This study discovers a synergistic effect when using a bipyridine covalent triazine framework (bipy-CTF) as support for an Ir^{III} complex in the aerobic oxidation reaction. The detailed mechanistic study provides insights into the function of the bipy-CTF in this synergistic catalysis. The EPR and in-situ XANES analyses confirm the applicability of bipy-CTF to activate oxygen and alcohol, resulting in an enhancement of the performance of the Ir^{III} complex to exceed the activity of the homogeneous counterpart. This is an unprecedented report on promoting the activity of a heterogeneous catalyst through its solid support.

1. Introduction

Oxidation reactions and more specifically the oxidation of alcohols to aldehydes still represents one of the most studied reactions, since aldehydes have significant importance both in academic research and industrial chemistry [1–4]. While traditional processes employ stoichiometric amounts of toxic and expensive inorganic oxidants [5], the quest for new catalytic systems employing environmentally benign reagents such as molecular oxygen is ongoing [6–10].

Many reports have appeared on the design of various catalysts containing late transition metals, such as Au, Pd, Pt and Ru enabling the aerobic oxidation of alcohols. These catalysts are limited by low selectivity and harsh reaction conditions [11–14]. Therefore, it is important to develop promoters within the reactions. Most of these examples feature a single promoter element, with bismuth being the most common [15–17]. Very recently, a mechanistic study demonstrated a clear promotional effect on the aerobic oxidative methyl esterification of alcohols by the addition of Bi and Te to a Pd catalyst on carbon support (PdBiTe/C) [18].

Amongst noble catalysts and attempts to enhance their catalytic activities, the chemistry and use of Ir are less explored. Since the initial successes with Ir^{III}Cp*-catalyzed (Cp* = 1,2,3,4,5-pentamethylcyclopentadienyl) aerobic oxidation of alcohols in 2006 [19], different homogeneous Ir-based catalysts were applied for alcohol oxidation using solely O_2 or air as green oxidant [20–23]. Mostly, these homogeneous catalysts exhibit fundamental drawbacks, such as low efficiency, in which high catalyst loadings are required as well as problems with catalyst recovery. A summary of these studies is presented in Table 1.

So far there is one report of a heterogeneous Ir catalyst for the

* Corresponding author.
E-mail address: Pascal.VanDerVoort@UGent.be (P. Van Der Voort).

https://doi.org/10.1016/j.apcatb.2020.118769
Received 8 May 2019; Received in revised form 23 January 2020; Accepted 15 February 2020
Available online 18 February 2020

Table 1
Selective aerobic/oxidant-free oxidation of benzyl alcohol catalyzed by homogeneous catalysts.

Catalyst	Reaction Conditions	Conv. Or Yield (%)	Ref.
$[Cp^*IrCl_2]_2$	5 mol% [Ir], Et_3N, 80 °C, 12 h, toluene, purged with O_2	82	[20]
Cp^*Ir(2-hydroxypyridine)Cl_2	1 mol% Ir, reflux in toluene, 20 h, oxidant-free (under Ar)	24	[21]
$[Cp^*IrCl_2]_2$	1 mol% [Ir], additive, toluene, 100 °C, 24 h, air	34	[22]
$[Ir(bipy)(H_2O)Cp^*](OTf)_2$	0.5 mol% Ir, 100 °C, 20 h, H_2O, oxidant-free (under Ar)	25	[23]
$[Ir(OH\text{-}bipy)(H_2O)Cp^*](OTf)_2$	1.5 mol% Ir, 100 °C, 20 h, H_2O, oxidant-free (under Ar)	92	[23]

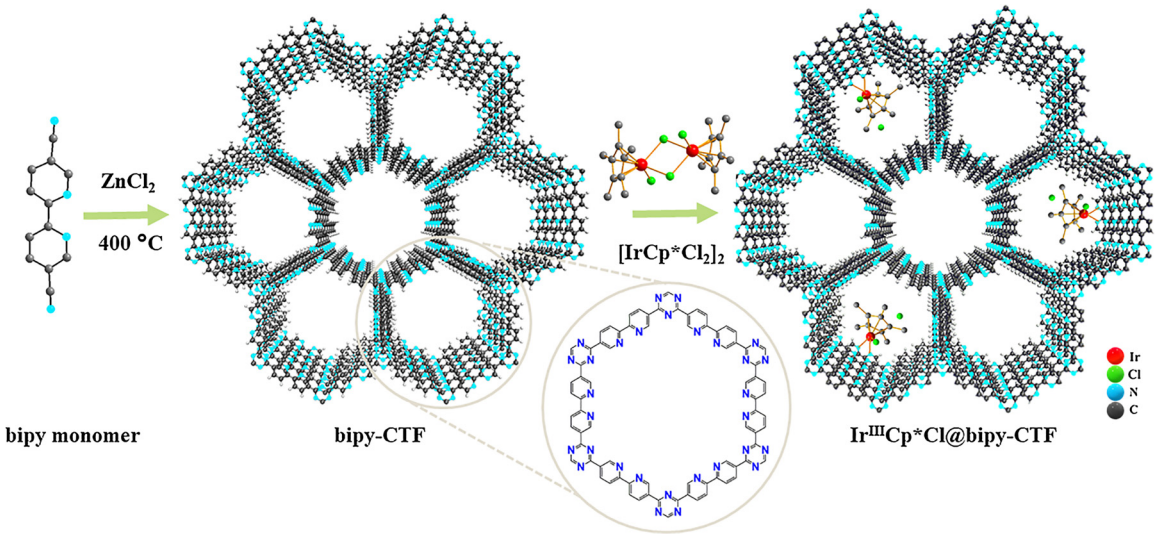

Scheme 1. Schematic representation of the ideal ordered structure of $Ir^{III}Cp^*Cl$@bipy-CTF catalyst.

aerobic oxidation of alcohols using supported iridium (oxide) nanoparticles on CeO_2 [24]. The activity of this catalyst for the selective oxidation of benzyl alcohol to benzaldehyde could be ascribed to the CeO_2 support and the iridium oxide centers (conversion ~55 %). We recently developed the immobilization of an Ir^{III} complex onto a metal-organic framework (MOF) support [25]. Catalytic results revealed that the presence of iodobenzene as co-oxidant was critical to achieve good conversions of benzyl alcohol (up to 54 %). Still, the MOF-based catalyst suffers from poor stability in aqueous acidic and basic media. Thus, a fundamental shift towards the development of much more stable support and more atom-efficient methods that use recyclable catalysts and molecular oxygen as the sole oxidant, without any sacrificial agent is highly desirable.

Covalent triazine frameworks (CTFs) possessing N-donor motifs belong to the most novel and advanced nanoporous supports to immobilize homogenous species [26,27]. Moreover, CTFs exhibit great thermal and chemical stabilities, large pore volumes, and high surface areas, making them ideal support for catalysis [28,29]. Within this context, Palkovits et al. [30]. developed a Pt-based catalyst using 2,6-dicyanopyridine as the monomer to construct the CTF. The N-rich CTF was employed to anchor a Pt precursor. The performance of the resulting catalyst was examined for methane oxidation to methanol using SO_3 in concentrated sulfuric acid. The $K_2[PtCl_4]$-CTF catalyst demonstrated a high turnover number (TON) around 300 even after five recycling steps. So far, the potential application of CTFs has been examined to design various heterogeneous catalysts containing (transition) metal complexes, such as Pd, Cu, Ni, Co, and Ru [27,31–34]. Accordingly, CTFs have proven to be highly stable materials and can be recycled easily. Besides these features, we discovered that the CTF does not only act as support for the Ir complex but also serves as a promoter that enhances the yield of the oxidation reaction compared to the homogeneous and heterogeneous Ir-based counterparts. The remarkable synergistic effect is a consequence of oxygen and alcohol activation assisted by the nitrogen-rich CTF. In order to investigate the promotional feature of the CTF as the catalyst support, we have undertaken a mechanistic study of $Ir^{III}Cp^*Cl$@bipy-CTF-catalyzed oxidation of benzyl alcohol. The results revealed the differences between the oxidation mechanisms of the heterogeneous catalyst and its homogeneous analog. To the best of our knowledge, this is the first report on the applicability of CTFs as the catalyst support and promoter in synergistic catalysis and participating effectively in the alcohol oxidation reaction.

2. Results and discussion

2.1. Synthesis and Characterization of the modified bipy-CTF with the Ir Complex ($Ir^{III}Cp^*Cl$@bipy-CTF)

The preparation of the targeted bipy-CTF material was achieved following the standard procedure described in the literature [35] applying the typical ionothermal conditions. The bipy-CTF was synthesized using the bipy linker (5,5′-dicyano-2,2′-bipyridine) in molten $ZnCl_2$ serving as both solvent and Lewis acid catalyst during the reaction. The bipy-CTF material contains numerous N moieties with free bipy sites which form excellent anchoring points for the grafting of the $[IrCp^*Cl_2]_2$ complex. A schematic view of the obtained structure is shown in Scheme 1.

Both bipy-CTF and $Ir^{III}Cp^*Cl$@bipy-CTF materials were characterized by X-ray diffraction (XRD), nitrogen sorption measurements, and elemental analysis. As for most of the CTFs, bipy-CTF was found to be predominantly amorphous. The broad peaks at 2θ ~ 13 and 25° were attributed to the [001] reflection indicating a “graphitic” layer stacking (Figure S2) [35]. Most of the CTFs synthesized under ionothermal conditions are of low crystallinity or even amorphous. Therefore, the detailed structural characterization of CTFs remains a huge challenge. Additionally, the relatively high temperature of synthesis inevitably leads to the partial carbonization. Within this context, we applied elemental analysis to estimate the carbonization degree. As shown in

Table 2
Elemental analysis, specific surface area, and total pore volume of pristine and modified CTF materials.

Sample	S_{BET} ($m^2\ g^{-1}$)	V_T^a ($cm^3\ g^{-1}$)	C[b] (Wt.%)	N[b] (Wt.%)	C/N	Ir[c] (mmol g^{-1})
bipy-CTF	787	0.40	58.92	20.27	2.9	–
Ir^{III}Cp*Cl@bipy-CTF	527	0.27	58.87	19.52	3.0	0.2

[a] Total pore volume at $p/p_0 = 0.99$.
[b] Determined by elemental analysis.
[c] Determined by ICP-OES analysis.

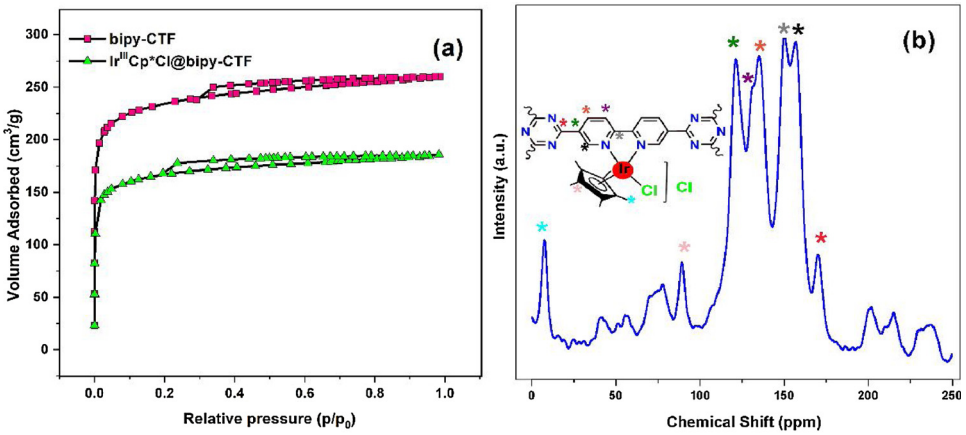

Fig. 1. (a) N_2 adsorption isotherms of the bipy-CTF and Ir^{III}Cp*Cl@bipy-CTF materials, (b) ^{13}C MAS solid-state NMR spectrum of Ir^{III}Cp*Cl@bipy-CTF (the peaks from 30-80 and 200-250 ppm correspond to the spinning sidebands).

Table 2, the CHN data obtained from the bipy-CTF material reveals a C/N ratio of 2.9 and the theoretical value for C/N in the bipy-CTF sample is calculated to be 2.6. This result confirms that partial carbonization of around 10 % occurs, while 90 % of the precursor composition is preserved.

As demonstrated in Fig. 1a, bipy-CTF displayed a rapid N_2 uptake at low relative pressures which is indicative of a highly microporous material (type I isotherm). The bipy-CTF exhibits a Brunauer–Emmett–Teller (BET) and Langmuir surface area of 787 and 1135 $m^2\ g^{-1}$ respectively. The total pore volume was found to be 0.40 $cm^3\ g^{-1}$ at $P/P_0 = 0.99$. The nitrogen adsorption isotherm of Ir^{III}Cp*Cl@bipy-CTF also exhibited a typical type I isotherm. The total pore volume was 0.27 $cm^3\ g^{-1}$ at $P/P_0 = 0.99$. After the introduction of the Ir complex, the surface area and pore volume decrease moderately due to the presence of the Ir complex (Table 2).

The thermal stability of the pristine and post-modified materials was determined by means of thermogravimetric analysis (TGA) and the results are presented in Figure S3. The TGA curve of the Ir^{III}Cp*Cl@bipy-CTF catalyst reveals a reduced thermal stability compared to bipy-CTF. The weight loss at around 190 °C is probably related to the loss of the Ir complex. The pristine bipy-CTF is thermally stable up to 500 °C.

To probe the local bonding environments of the immobilized iridium complex, ^{13}C MAS solid-state NMR measurements were performed. As shown in Fig. 1b, the ^{13}C spectrum of Ir^{III}Cp*Cl@bipy-CTF exhibits six well-resolved signals at 121, 132, 136, 151, 159, and 170 ppm which correspond to those reported by Hug et al. [35] for the bipy-CTF material. Moreover, the appearance of two additional peaks at 89 and 8 ppm is characteristic of the presence of the C_5Me_5 group of the Ir complex [36]. Further evidence for the successful attachment of the half-sandwich Ir^{III}Cp* complex onto the bipy-CTF was achieved by XPS analysis (Figure S4) and results are provided in the SI. Additionally, EXAFS analysis was performed to determine the coordination of the Ir complex to the bipy-CTF material. It was found that for the complex before and after catalysis, the Ir^{III}Cp*Cl@bipy-CTF is characterized by an Ir–N bond distance of 2.11 Å (Table 3, S1, Figure S5). This experimentally determined bond distance is in agreement with the theoretically calculated distances for the Ir complexation onto the bipyridine moiety (~2.092 Å and ~2.086 Å at the M06 and B3LYP levels of theory, respectively, Table 3, Figure S6 and Table S2). As such, both methods corroborate that the Ir complex is coordinated to the N atoms of the bipyridine sites.

Table 3
Bond distance results of the Ir^{III}Cp*Cl@bipy-CTF material determined by experimental and computational structural data on a model composed by Ir^{III}Cp*Cl@bipy-CTF. The bipy-CTF part is composed of two bipy and three triazine groups as shown in Figure S1 of the Supporting Information.

Coordinated atoms	Bond lengths		
	[a]	[b]	[c]
Ir^{3+}–N (bipy)	2.114 Å	2.092 Å	2.086 Å
Ir^{3+}–C (Cp*)	2.2619 Å	2.244 Å	2.257 Å

(a) EXAFS fit results, (b) M06, (c) B3LYP levels of theory in combination with the LanL2-DZ basis combined basis set and pseudopotential.

ADF-STEM imaging (Fig. 2a) was exploited to investigate the morphology and the crystallinity of the bipy-CTF. The material consists of agglomerated amorphous nanosheets of ~10−15 nm in size with some crystalline patches embedded. Dark contrast features marked by the white arrows correspond to the pores of ~2−3 nm in diameter. The Fourier transform pattern contains hexagonally arranged reflections with ~2.5 Å spacing. Additionally, from TEM images (Figure S7), the layered morphology of bipy-CTF is obvious. A homogeneous distribution of elements within the Ir^{III}Cp*Cl@bipy-CTF is important for its use in catalysis. From the EDX images presented in Fig. 2b, a homogeneous distribution of C and N elements is observed. Moreover, elemental mapping revealed a homogeneous distribution of Ir and Cl elements.

2.2. Comparison of [Ir^{III}(bipy)Cp*Cl]Cl and Ir^{III}Cp*Cl@bipy-CTF catalysts in the selective oxidation of benzyl alcohol

The selectivity control towards aldehyde in the aromatic alcohol

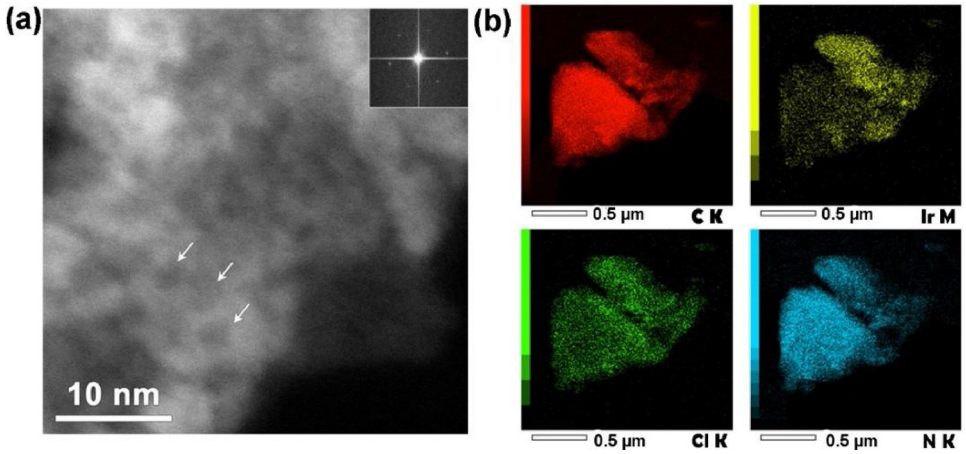

Fig. 2. (a) ADF-STEM image of the bipy-CTF material together with the corresponding Fourier transform pattern shown in the inset, (b) EDX elemental mapping images for $Ir^{III}Cp^*Cl$@bipy-CTF.

Table 4
Catalytic performance of different catalysts in the oxidation of benzyl alcohol.

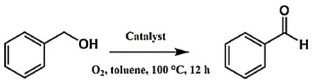

Entry	Catalyst (mol%[a] or mg)	Conversion[b] (%)	TON[c]
1	$Ir^{III}Cp^*Cl$@bipy-CTF (0.24 mol%)	57	237.5
2	$Ir^{III}Cp^*Cl$@bipy-CTF (0.5 mol%)	65	130
3	$Ir^{III}Cp^*Cl$@bipy-CTF (1 mol%)	99	99
4	No catalyst	< 1	–
5[d]	$Ir^{III}Cp^*Cl$@bipy-CTF (1 mol%)	7	–
6[e]	$Ir^{III}Cp^*Cl$@bipy-CTF (1 mol%)	< 1	–
7[f]	$Ir^{III}Cp^*Cl$@bipy-CTF (1 mol%)	46	46
8[f]	bipy-CTF (17 mg)	< 1	–
9[g]	bipy-CTF (17 mg)	39	–
10[h]	bipy-CTF (17 mg)	39	–
11[i]	$Ir^{III}Cp^*Cl$@COMOC-4 (1 mol%)	38	39.6
12	$Ir^{III}Cp^*Cl$@bipy-CTF$^{2nd\ run}$ (1 mol%)	99	99
13	$Ir^{III}Cp^*Cl$@bipy-CTF$^{3rd\ run}$ (1 mol%)	97	97
14	$Ir^{III}Cp^*Cl$@bipy-CTF$^{4th\ run}$ (1 mol%)	97	97
15	$Ir^{III}Cp^*Cl$@bipy-CTF$^{5th\ run}$ (1 mol%)	97	97
16	$Ir^{III}Cp^*Cl$@bipy-CTF$^{6th\ run}$ (1 mol%)	97	97
17	$Ir^{III}Cp^*Cl$@bipy-CTF$^{7th\ run}$ (1 mol%)	97	97

Reaction conditions: 0.33 mmol benzyl alcohol, 0.4 mmol Cs_2CO_3, 330 µl toluene, O_2, 100 °C, 12 h.

[a] based on Ir ion calculated from ICP-OES analysis.

[b] Conversions are an average of at least three runs.

[c] mmol of product formed per mmol of Ir in the catalyst.

[d] The reaction was done under Ar atmosphere.

[e] The reaction was done in the absence of Cs_2CO_3.

[f] *p*-benzoquinone (0.33 mmol) was added.

[g] *tert*-butyl alcohol (0.33 mmol) was added.

[h] NaN_3 (0.33 mmol) was added.

[i] The obtained results from ref. [25], Temp. 150 °C and in the presence of iodobenzene as co-oxidant.

* All catalysts displayed > 99 % selectivity towards benzaldehyde.

oxidation using molecular oxygen under mild conditions remains a great challenge. To test the applicability of the heterogeneous catalyst, we first selected the oxidation of benzyl alcohol as this is the substrate of choice in many reports on Ir catalyzed oxidation reactions. For the purposes of comparison, toluene was selected as the reaction medium similar to the reports on homogeneous and heterogeneous Ir catalysts in aerobic alcohol oxidation [20–22,24]. The catalytic performance of the obtained $Ir^{III}Cp^*Cl$@bipy-CTF material was evaluated in the selective oxidation of benzyl alcohol to benzaldehyde using O_2 as the stoichiometric oxidant. The catalytic results are listed in Table 4.

We found that the heterogeneous $Ir^{III}Cp^*Cl$@bipy-CTF catalyst presents the highest activity yet reported for this aerobic transformation (in terms of conversion and reaction time, either homogeneously or heterogeneously). A comparison of these results with those reported for the homogeneous Ir-based catalysts (Table 1) clearly illustrates the enhanced catalytic efficiency of the $Ir^{III}Cp^*Cl$@bipy-CTF catalyst since much less catalyst (1 mol% Ir) is required to provide a much higher conversion of benzyl alcohol (99 %). It is important to note that the product of over-oxidation (benzoic acid) was not detected, showcasing the high selectivity of the Ir-based catalyst towards benzaldehyde. In an attempt to explore the role of the applied base, different bases were examined. The conversion of benzyl alcohol improves in the presence of Cs_2CO_3, however, in the presence of K_2CO_3 and Na_2CO_3 a reduced activity was observed with conversions of 75 and 43 % towards benzyl alcohol. To understand the catalytic behavior of our heterogeneous catalyst, we tested the catalytic activity of its homogeneous counterpart. The $[Ir^{III}(bipy)Cp^*Cl]Cl$ complex, tested under the same reaction conditions, resulted in a remarkably lower conversion of benzyl alcohol (42 %) as shown in Fig. 3. We also compared the use of a bipyridine linker MOF (COMOC-4) instead of the CTF in the same reaction conditions [25]. When the same Ir complex was immobilized on COMOC-4 as the solid support, the oxidation of benzyl alcohol proceeded slowly and a conversion of 38 % was observed after 24 h under similar reaction conditions (Fig. 3). Moreover, the presence of iodobenzene as the co-oxidant was vital in our previously reported $Ir^{III}Cp^*Cl$@COMOC-4 catalyst and can be avoided here. In order to make a fair comparison of the activity of the catalysts, we calculated the highest possible turnover number (TON) for all catalysts based on the Ir centers as the active site. While a high TON of 237.5 was obtained using 0.24 mol% $Ir^{III}Cp^*Cl$@bipy-CTF catalyst, the $[Ir^{III}(bipy)Cp^*Cl]Cl$ (1 mol%) and $Ir^{III}Cp^*Cl$@COMOC-4 (1 mol%) catalysts resulted in a remarkably lower TON (Fig. 3). These observations indicate that the high catalytic performance of the $Ir^{III}Cp^*Cl$@bipy-CTF catalyst can be ascribed to the CTF as the solid support.

2.3. Promotional effect of bipy-CTF as support for the enhanced catalytic performance of $Ir^{III}Cp^*Cl$@bipy-CTF catalyst

In order to elucidate the cause of the enhanced catalytic activity, a control experiment was performed using the pristine bipy-CTF. Interestingly, a conversion of 39 % was obtained under identical reaction conditions at 100 °C (Fig. 3). This so far not discovered activity for bipy-CTF is comparable with the previously reported catalytic activities for nitrogen-doped carbon materials [37–42]. It is well-known that various nitrogen-doped carbon materials have the potential to act as effective catalysts for aerobic oxidation reactions [37–44]. According

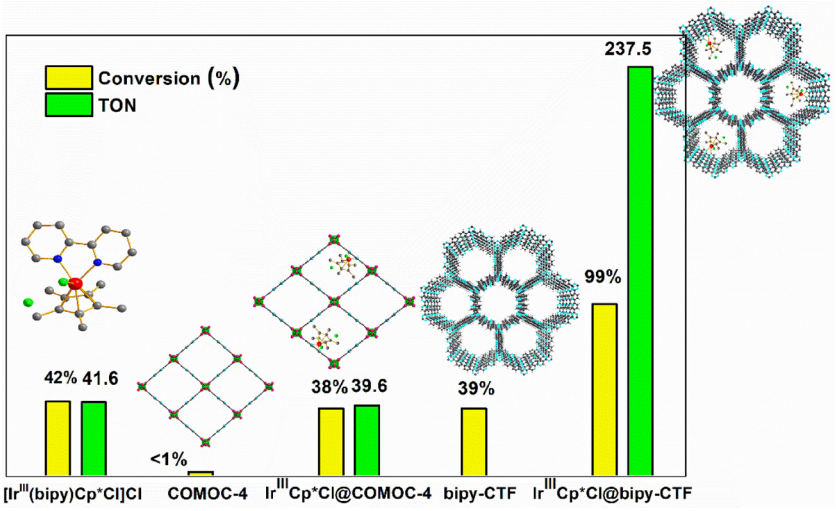

Fig. 3. Comparison of the catalytic activities of COMOC-4, bipy-CTF and a series of Ir-based catalysts with different catalyst supports for the alcohol oxidation (Reaction conditions: 0.33 mmol benzyl alcohol, 17 mg catalyst (COMOC-4, bipy-CTF) or 1 mol% Ir (Ir-based catalysts), 0.4 mmol Cs_2CO_3, 330 μL toluene, O_2). TON is calculated based on 0.24 mol% $Ir^{III}Cp^*Cl$@bipy-CTF and 1 mol% $Ir^{III}Cp^*Cl$@COMOC-4 catalysts. For COMOC-4 and $Ir^{III}Cp^*Cl$@COMOC-4, the reactions are done at 150 °C for 24 h and in the presence of iodobenzene as co-oxidant. For bipy-CTF, $[Ir^{III}(bipy)Cp^*Cl]Cl$ and $Ir^{III}Cp^*Cl$@bipy-CTF, the reactions are done at 100 °C for 12 h.

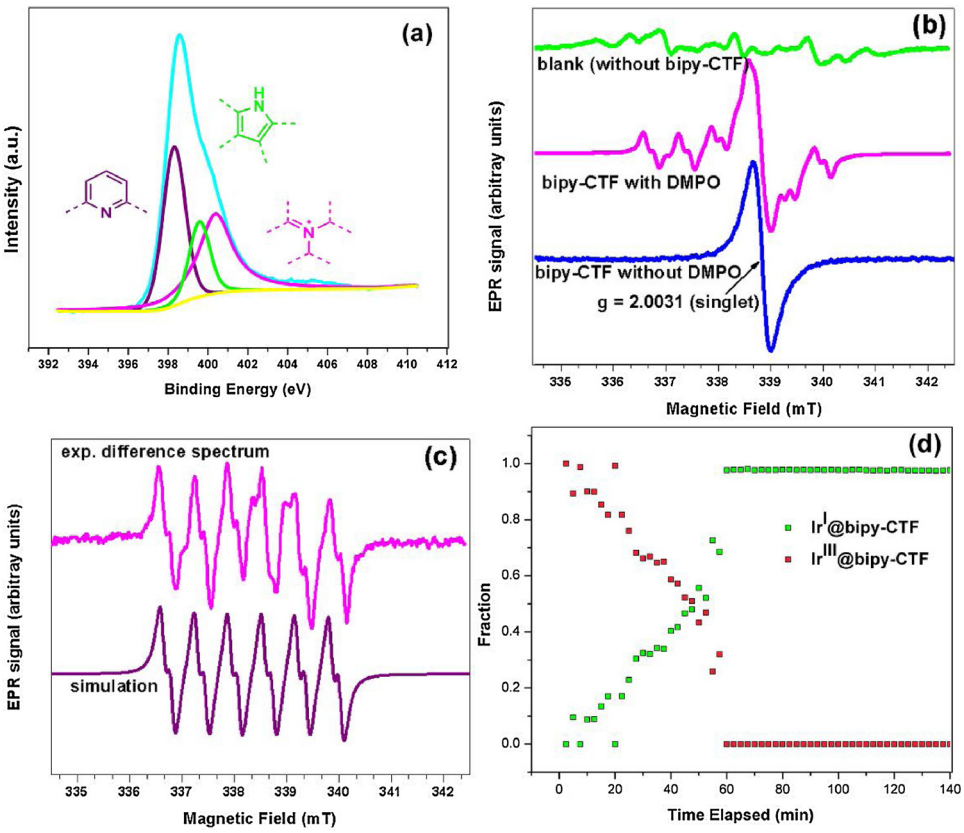

Fig. 4. (a) N 1s XPS spectra of the bipy-CTF, (b) EPR spectra of blank (DMPO in the reaction mixture without bipy-CTF), bipy-CTF with and without DMPO, (c) For clarification the bipy-CTF without DMPO spectrum is eliminated from that of the solution containing both the CTF and the spin trap, (d) XANES linear combination fit results of the in-situ catalytic run using O_2 as the oxidant (a clear transition of an Ir^{III} to Ir^{I} state occurs as a function of reaction time).

to these studies, nitrogen moieties in different electronic environments are formed on the surface of nitrogen-doped carbon materials such as pyridinic N, pyrrolic N and graphitic N. The graphitic sp^2 N atoms were established to be the catalytically active centers for aerobic oxidation reactions. It should be noted that CTFs are synthesized by the trimerization of aromatic nitriles at elevated temperatures and various side reactions can occur under these conditions. However, the effect of these side reactions on the properties of materials is rarely discussed. Recently, Osadchii et al. [45] have successfully assigned a number of nitrogen functionalities in CTFs by using X-ray photoelectron spectroscopy (XPS). Similarly, the XPS surface characterization of the bipy-CTF material in this study demonstrates the existence of three different types of nitrogen functionalities: pyridinic (398.5 eV), pyrrolic (400 eV), and graphitic (401 eV) nitrogen species (Fig. 4a). Since the catalytic activity of the $Ir^{III}Cp^*Cl$@bipy-CTF catalyst is higher even than the sum activities for the homogeneous $[Ir^{III}(bipy)Cp^*Cl]Cl$ (42 %) and the heterogeneous bipy-CTF catalysts (39 %), we discovered an unusual synergistic effect between the Ir metal centers and the bipy-CTF support. To explain this phenomenon, we have undertaken a mechanistic study of the $Ir^{III}Cp^*Cl$@bipy-CTF-catalyzed oxidation of benzyl alcohol.

2.4. Mechanistic proposal for the aerobic oxidation of alcohols over $Ir^{III}Cp^*Cl$@bipy-CTF

To gain mechanistic insight into the selective aerobic oxidation reaction, we performed a series of control experiments. From the results summarized in Table 4, we observed that no product was formed in the

absence of the catalyst or base (entries 4 and 6). Furthermore, the conversion of benzyl alcohol towards benzaldehyde dramatically lowered to 7 % under Ar atmosphere, proving the essential role of oxygen as the oxidant (entry 5 in Table 4). The addition of *p*-benzoquinone as superoxide ($^{\bullet}O_2^-$) scavenger into the reaction system containing bipy-CTF as the catalyst, completely suppressed the oxidation of benzyl alcohol (conversion < 1%, Table 4, entry 8 cf. Fig. 3). This observation indicates that bipy-CTF activates molecular oxygen to superoxide, which acts as oxidant species in the catalytic cycle. In order to elucidate whether other activated oxygen species are created in our system or not, different scavengers including *tert*-butyl alcohol and NaN_3 were introduced into the reaction mixture to particularly inhibit the generation of $^{\bullet}OH$ and $^1O_2$ respectively. In these cases, no reduction in the catalytic activities was observed (entries 9 and 10 in Table 4). The obtained data provide an explanation for the great selectivity of our oxidation system towards aldehydes since $^{\bullet}OH$ is identified as a strong non-selective oxidant. Another control experiment was conducted with *p*-benzoquinone in the presence of the Ir^{III}Cp*Cl@bipy-CTF catalyst. Upon the addition of *p*-benzoquinone, the conversion of benzyl alcohol was notably inhibited to 46 % which is almost identical to the homogeneous [Ir^{III}(bipy)Cp*Cl]Cl catalyst. The fact that the oxidation reaction is not completely hindered by *p*-benzoquinone implies that a different oxidation pathway without the production of superoxide exists involving the Ir catalytic centers. Accordingly, it can be concluded that the Ir centers of the catalyst are not capable to activate oxygen in the reaction system and therefore, the oxygen activation most probably proceeds on the bipy-CTF as the catalyst support. This is in accordance with the mechanism proposed by Gabrielsson et al. [19] for the [Ir^{III}(bipy)Cp*Cl]Cl-catalyzed aerobic oxidation of benzyl alcohol showing the role of molecular oxygen only in the last step of the cycle for the regeneration of Ir^{III} from the Ir^{I} intermediate (Figure S8).

To gain a deeper insight into the promotional role of the bipy-CTF as support, the mechanistic investigations outlined above were complemented by Electron Paramagnetic Resonance (EPR) analyses. To identify the generated active oxygen species in our catalytic system, 5,5-dimethyl-1-pyrroline *N*-oxide (DMPO) was used as the trapping agent. As shown in Fig. 4b, there is only a very weak EPR signal in the absence of the bipy-CTF catalyst (top trace). For the reaction mixture containing bipy-CTF, a clear change of the EPR signals is revealed. Without DMPO (bottom trace), the EPR spectrum of the reaction mixture containing bipy-CTF is a strong singlet at g = 2.0031, with a Lorentzian line shape and a peak-to-peak width of 0.33 mT. This CTF radical and its EPR characteristics will be discussed in more detail in a forthcoming paper. In the presence of DMPO, an extra sextet appears (middle trace). By a numerical elimination of the CTF singlet, a sextet spectrum, in which each line shows an additional small splitting, can be quite successfully isolated (Fig. 4c, top trace). The latter spectrum can be convincingly assigned to an alkoxyl DMPO adduct. Indeed, a spectrum simulation using the spin Hamiltonian parameters published by Buettner [46] for this type of adduct in a toluene solvent, as is the case here, exhibits a striking agreement with experiment (g = 2.0061 ; a_N = 1.284 mT (^{14}N), A_{H1} = 0.648 mT (^{1}H), A_{H2} = 0.168 mT (^{1}H), Lorentzian peak-to-peak linewidth = 0.27 mT).

The identification of the involved radical as $PhCH_2O^{\bullet}$-DMPO, confirms the role of bipy-CTF in the activation of benzyl alcohol. Based on the observations from the control experiments, we propose that the generated superoxide on the surface of bipy-CTF reacts with benzyl alcohol to generate $PhCH_2O^-$ and subsequently $PhCH_2O^{\bullet}$. The obtained results thus corroborate each other, unveiling the promotional impact of bipy-CTF in activating oxygen and benzyl alcohol in our reaction system. More specifically, the generated $PhCH_2O^{\bullet}$ on the surface of bipy-CTF reacts with the Ir centers in the reaction system. Accordingly, in the mechanism for the heterogeneous Ir^{III}Cp*Cl@bipy-CTF-catalyzed aerobic oxidation of benzyl alcohol, the step for the deprotonation to an alkoxide complex is removed compared to the homogeneous Ir^{III}Cp*Cl@bipy-CTF catalyst. Therefore, bipy-CTF serves as a promoter that enhances the yield of the oxidation reaction compared to the homogeneous counterparts.

From the experimental results, we derive three plausible reaction pathways that explain the role of the Ir centers, the bipy-CTF support and their combined effect.

In order to understand the function of the Ir complex during catalysis, we refer to the mechanism reported by Gabrielsson et al. [19] which is shown in Figure S8. Additionally, we employed in-situ XANES that nicely proves a shift in the Ir oxidation state from the Ir^{III}@bipy-CTF to an Ir^{I}@bipy-CTF state (Fig. 4d). This observation is in good agreement with the plausible mechanistic pathway in the literature [19] involving an Ir^{I}/Ir^{III} cycle. Therefore, we can conclude that the selective oxidation of benzyl alcohol via some of the Ir centers in our heterogeneous catalyst can proceed similarly.

Besides this pathway, we discovered a new activity of the bipy-CTF in the oxidation of benzyl alcohol. Our findings suggest that this activity possibly originates from the oxygen activation on the surface of CTF, which is a key step in oxidation reactions. Although the active sites and the mechanism have not yet been completely understood, graphitic sp^2 N atoms were established to be the catalytically active centers for aerobic oxidation reactions using various nitrogen-doped carbon materials [37]. Nitrogen doping facilitates the adsorption of O_2 on carbon-based materials. Accordingly, molecular oxygen dissolved in the liquid phase is adsorbed on a carbon site adjacent to the graphitic N and/or on the carbon atom and the N atom which results in the formation of superoxide radicals. The most likely mechanism is proposed based on the obtained results and previous studies [37,47], as shown in Scheme 2.

The above investigations have indicated that both the Ir centers and bipy-CTF are critical for the remarkable activity in the oxidation reaction. More importantly, our heterogeneous catalyst presented much higher catalytic activity even than the sum activities of the homogeneous Ir catalyst and bipy-CTF. The fact that many heterogeneous catalysts demonstrate similar or even lower catalytic activities compared to their homogeneous counterparts is another clue clearly reinforcing the presence of an unusual synergistic effect in the catalytic process boosting the catalytic activity of the Ir centers.

In order to obtain more insight into the role of the base, the influence of different bases was investigated in the presence of bipy-CTF, homogeneous [Ir^{III}(bipy)Cp*Cl]Cl and Ir^{III}Cp*Cl@bipy-CTF catalysts. The obtained results are summarized in Table S3. As can be observed, the reaction without any basic additive resulted in no conversion of benzyl alcohol (Table S3, entry 1). However, the addition of a variety of bases, such as Na_2CO_3, K_2CO_3, and Cs_2CO_3, considerably improved the catalytic activity of the catalysts, with the highest activity obtained using Cs_2CO_3 (Table S3, entries 4, 7 and 11). This difference in the activity is due to the stronger basicity of Cs_2CO_3 compared to other alkali carbonates. We believe that the addition of base to the mixture containing the [Ir^{III}(bipy)Cp*Cl]Cl catalyst can facilitate the deprotonation of benzyl alcohol in the [Cp*Ir($OHCH_2Ph$)(bipy)] to form the corresponding alkoxide compound. Additionally, the base may aid with the deprotonation of the $[Cp^*Ir(H)(bipy)]^+$ to generate a Cp*Ir(bipy) intermediate. We assume that Cs_2CO_3 may also assist the formation of the alkoxy intermediate in the catalytic cycle of the bipy-CTF catalyst.

With this information at hand, the mechanism building upon the promotional effect between the bipy-CTF as support and Ir metal centers is depicted in Scheme 2. As we explained, benzyl alcohol converts into its anionic form on the surface of bipy-CTF. Subsequently, the substitution of the halide proceeds by the activated substrate ($PhCH_2O^-$). Moreover, in this pathway, the deprotonation step giving the alkoxide complex is removed compared to the original mechanism by the homogeneous catalyst (Figure S8) due to the direct coordination of $PhCH_2O^-$ to the Ir centers. The β-hydride elimination from the alkoxide complex rapidly gives a hydride which further generates Cp*Ir(bipy) through deprotonation. Oxidation followed by the addition of benzyl alcohol anion (or benzyl alcohol) regenerates the alkoxide complex.

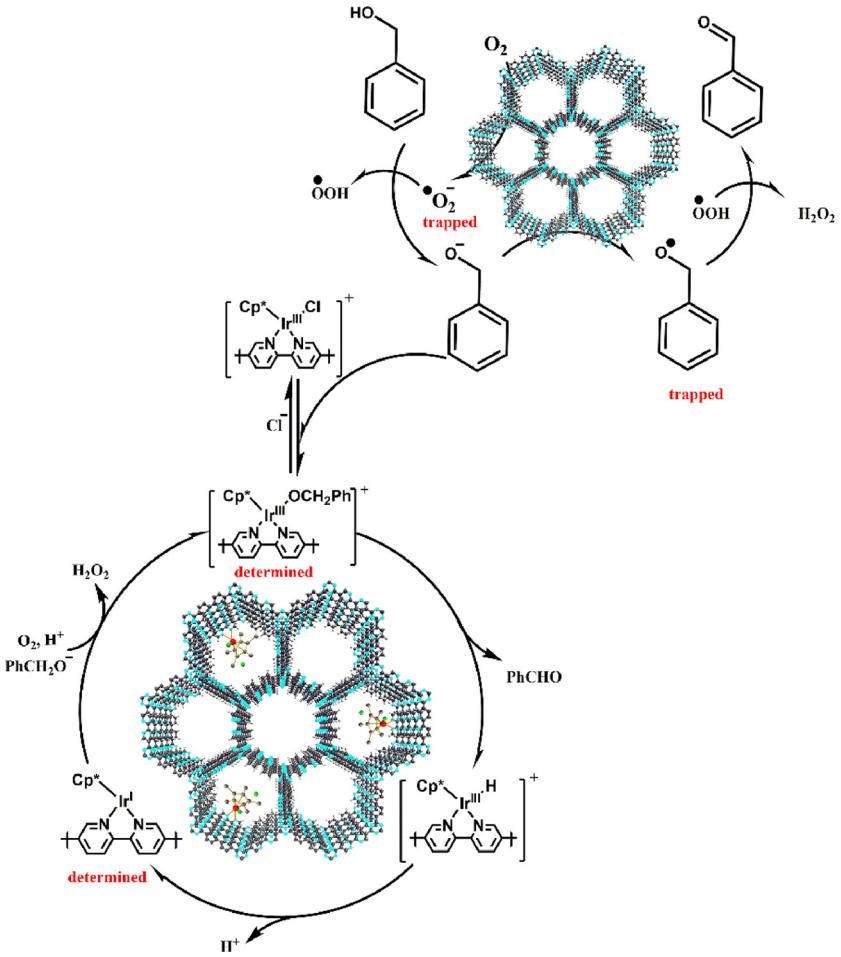

Scheme 2. Proposed mechanism for the Ir^{III}Cp*Cl@bipy-CTF-catalyzed aerobic oxidation of benzyl alcohol.

2.5. Substrate scope studies over Ir^{III}Cp*Cl@bipy-CTF

Inspired by the superior catalytic performance of Ir^{III}Cp*Cl@bipy-CTF in the oxidation of benzyl alcohol, we proceeded to examine the scope of this reaction. Various substituted benzyl alcohols were oxidized and the obtained results are listed in Table 5, entries 1-5. In general, the catalyst showed high activity for both types of substrates (electron-withdrawing and electron-donating) as well as complete selectivity towards the related aldehydes over carboxylic acid. However, a reduced activity was observed for cinnamyl alcohol (Table 5, entry 6) which might be due to the steric hindrance during the substrate coordination step. In the presence of different aromatic alcohols (entries 7–10), still, a good conversion was obtained. As can be observed from Table 5, entries 11–12, the catalyst shows good catalytic activity for the conversion of secondary alcohols towards the related ketones. Compared to aromatic alcohols, aliphatic/allylic alcohol substrates (entries 13–15) react more sluggishly and afford only moderate conversions (10–22 %). The Ir^{III}Cp*Cl@bipy-CTF catalyst exhibits a comparable catalytic performance towards the oxidation of aliphatic alcohols in terms of TON compared to the homogeneous $[Cp^*IrCl_2]_2$ catalyst reported previously [20].

2.6. Recyclability studies of Ir^{III}Cp*Cl@bipy-CTF

After catalysis, the Ir^{III}Cp*Cl@bipy-CTF catalyst could be easily recovered by simple filtration. The recyclability of the catalyst was examined showing that the Ir^{III}Cp*Cl@bipy-CTF catalyst could be reused at least seven times without significant loss of activity and selectivity (Table 4 entries 12–17). In addition, the filtrate obtained after the recovery of the catalyst was analyzed by means of ICP-OES showing no detectable Ir leaching (0.05 ppb). This supports the existence of a strong interaction between the Ir complex and bipy-CTF. The distribution of the elements within the recycled Ir^{III}Cp*Cl@bipy-CTF after the first run was investigated using EDX analysis. As shown in Figure S9, the distribution of the elements remains similar to that of the fresh Ir^{III}Cp*Cl@bipy-CTF.

2.7. Environmentally friendly alcohol oxidation over Ir^{III}Cp*Cl@bipy-CTF

The development of a highly efficient and green system for the selective oxidation of alcohols without using toxic oxidants is an important and highly challenging area in organic chemistry and particularly in the chemical industry. Inspired by the great activity of the Ir^{III}Cp*Cl@bipy-CTF catalyst in the aerobic oxidation of alcohols, we proceeded to examine the wide applicability of this catalyst under environmentally friendly conditions (Table 6). For this purpose, water and ethyl acetate were selected to be applied as the reaction medium. The experiments revealed the high efficiency of the catalyst exhibiting a great conversion of 89 % and 99 % using ethyl acetate and water respectively with complete selectivity towards benzaldehyde. The catalytic reaction was also performed under solvent-free conditions using 10 times more amount of benzyl alcohol. Interestingly, a high conversion of 71 % was observed with a high TON of 689. Additionally, the Ir^{III}Cp*Cl@bipy-CTF material is an efficient catalyst for the oxidation of benzyl alcohol using air as the oxidant instead of O_2. By using 1 bar of air as the oxidant, 99 % of benzyl alcohol was converted after 12 h of reaction with the same selectivity. It is important to note that by reducing the reaction temperature to 80 and 50 °C, still high conversions

Table 5
Catalytic performance of the $Ir^{III}Cp^*Cl$@bipy-CTF catalyst towards the oxidation of various substrates.

Entry	Substrate	Conversion (%)/TON	Selectivity (%)
1	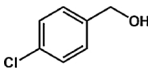	80/80	> 99
2	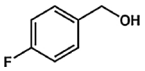	99/99	> 99
3	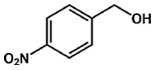	99/99	> 99
4	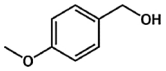	99/99	> 99
5	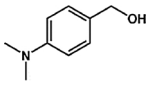	90/90	> 99
6	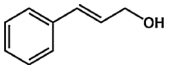	65/65	> 99
7	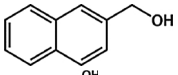	55/55	> 99
8	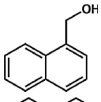	50/50	> 99
9	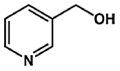	78/78	> 99
10	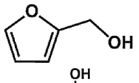	32/32	> 99
11	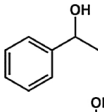	42/42	> 99
12	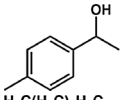	38/38	> 99
13	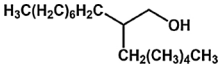	22/22	> 99
14	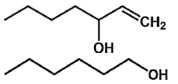	10/10	> 99
15	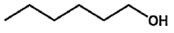	14/14	> 99

Reaction conditions: 1 mol% catalyst (based on Ir ion calculated from ICP-OES analysis), 0.33 mmol alcohol, 0.4 mmol Cs_2CO_3, 330 μL toluene, O_2, 100 °C, 12 h.

of 99 and 75 % were obtained. It is important to note that, all of the catalytic experiments in this work were performed on a small scale to reduce the amount of produced waste. However, to evaluate the applicability of the catalytic system, a scaled-up reaction was performed. Increasing the scale of the catalytic reaction up to 20 times more exhibits a full conversion of benzyl alcohol (99 %) with 99 % selectivity towards benzaldehyde, which is similar to the obtained results on a small scale.

3. Conclusions

Aiming at highly attractive synergistic strategies in heterogeneous catalysis, we unveil the activity of a CTF support with the capability of activating O_2. The reactions proceed with great selectivity and yield under mild conditions, while the catalyst can be recycled at least seven times without noticeable loss of activity. We discovered an unusual synergistic effect between the CTF support and the anchored Ir complex. We assign the excellent performance of the $Ir^{III}Cp^*Cl$@bipy-CTF catalyst to the combined roles of the bipy-CTF (activation of oxygen and

Table 6
Catalytic performance of the $Ir^{III}Cp^*Cl$@bipy-CTF catalyst under more environmentally friendly conditions.

	Reaction conditions				
Entry	Solvent	Oxidant	Temp. (°C)	Conversion (%)	TON
1	Ethyl acetate	O_2	100	89	89
2	Water	O_2	100	99	99
3	–	O_2	100	71	689
4	Water	Air	100	99	99
5[a]	Water	–	100	5	5
6	Toluene	Air	100	99	99
7	Toluene	O_2	80	99	99
8	Toluene	O_2	50	75	75
9	–	Air	100	20	194
10[b]	Water	O_2	100	99	99

Reaction conditions (for entries 1–2, 4–8 and 10): 1 mol% catalyst (based on Ir ion calculated from ICP-OES analysis), 0.33 mmol alcohol, 0.4 mmol Cs_2CO_3, 330 μL solvent, O_2/Air (1 bar), 12 h. Reaction conditions (for entries 3 and 9): 0.1 mol% catalyst (based on Ir ion calculated from ICP-OES analysis), 3.3 mmol alcohol, 0.8 mmol Cs_2CO_3, oxidant (1 bar), 12 h.

[a] The reaction is done under Ar atmosphere.

[b] The catalyst is reused for the 2nd run.

substrate) and the Ir centers (adsorption of the activated substrate). Among all homogeneous and heterogeneous Ir-based catalysts explored, $Ir^{III}Cp^*Cl$@bipy-CTF demonstrated the best performance for the aerobic oxidation of benzylic alcohols. This study represents one of the rare mechanistic reports on the promoted catalytic alcohol oxidation through the assistance of both metal centers and catalyst support representing molecular and radical mechanistic pathways to be involved in the reaction system.

Author contributions

PVDV and YYL conceived the project. SA and PGD synthesized the catalysts and performed the characterization and catalytic experiments. LV conceived the X-ray absorption spectroscopy experiments which was performed by PT and KL. FMM and VVS performed the calculations. YYL carried out NMR analyses. CS, JE and FVB conceived and performed organic syntheses. MM performed the ADF-STEM imaging. HV and FC conceived and performed the EPR experiments. All authors interpreted the data and contributed to the preparation of the manuscript.

Declaration of Competing Interest

The authors declare no competing financial interest.

Acknowledgments

SA acknowledges the financial support from the Ghent University BOF doctoral grant 01D04318. SA and PGD gratefully acknowledge the financial support from the Research Foundation Flanders (FWO-Vlaanderen) grant No. G000117N. PT also wishes to acknowledge FWO-Vlaanderen for financial support (grant 12Q7718N). KL thanks the financial support from the Ghent University. YYL thanks the financial support of the Ministry of Science and Technology, China (2016YFE01069800) and National Natural Science Foundation of China (21403025). JE, VVS and FM-M acknowledge the Fund for Scientific Research - Flanders (FWO) and the Research Board of Ghent University (BOF) for funding. Furthermore, we would like to acknowledge the DUBBLE staff for their support during the experiments, as well as the NWO and FWO for their continued financial support to the ESRF. We are grateful to Johannes Schmidt for the XPS analysis and Vitaliy Bliznuk for the experimental help with the STEM measurements. The authors thank the support from the Research Board of Ghent University (GOA010-17, BOF GOA2017000303). The computational resources and

services used were provided by the Flemish Supercomputer Center (VSC), funded by the Research Foundation: Flanders (FWO).

Appendix A. Supplementary data

Supplementary material related to this article can be found, in the online version, at doi:https://doi.org/10.1016/j.apcatb.2020.118769.

References

[1] C.H. Bai, A.Q. Li, X.F. Yao, H.L. Liu, Y.W. Li, Efficient and selective aerobic oxidation of alcohols catalysed by MOF-derived Co catalysts, Green Chem. 18 (2016) 1061–1069.

[2] R.A. Sheldon, I.W.C.E. Arends, A. Dijksman, New developments in catalytic alcohol oxidations for fine chemicals synthesis, Catal. Today 57 (2000) 157–166.

[3] H. Miyamura, R. Matsubara, Y. Miyazaki, S. Kobayashi, Aerobic oxidation of alcohols at room temperature and atmospheric conditions catalyzed by reusable gold nanoclusters stabilized by the benzene rings of polystyrene derivatives, Angew. Chemie Int. Ed. English 46 (2007) 4151–4154.

[4] D.I. Enache, J.K. Edwards, P. Landon, B. Solsona-Espriu, A.F. Carley, A.A. Herzing, M. Watanabe, C.J. Kiely, D.W. Knight, G.J. Hutchings, Solvent-free oxidation of primary alcohols to aldehydes using Au-Pd/TiO2 catalysts, Science 311 (2006) 362–365.

[5] Y.X. Liu, G.F. Zhao, D.S. Wang, Y.D. Li, Heterogeneous catalysis for green chemistry based on nanocrystals, Sci. Rev. 2 (2015) 150–166.

[6] C. Li, Chiral synthesis on catalysts immobilized in microporous and mesoporous materials, Catal Rev 46 (2004) 419–492.

[7] A.P. Wight, M.E. Davis, Design and preparation of organic-inorganic hybrid catalysts, Chem. Rev. 102 (2002) 3589–3613.

[8] C. Parmeggiani, C. Matassini, F. Cardona, A step forward towards sustainable aerobic alcohol oxidation: new and revised catalysts based on transition metals on solid supports, Green Chem. 19 (2017) 2030–2050.

[9] P. McMorn, G.J. Hutchings, Heterogeneous enantioselective catalysts: strategies for the immobilisation of homogeneous catalysts, Chem. Soc. Rev. 33 (2004) 108–122.

[10] L.Q. Liu, T.D. Dao, R. Kodiyath, Q. Kang, H. Abe, T. Nagao, J.H. Ye, Plasmonic janus-composite photocatalyst comprising Au and C-TiO2 for enhanced aerobic oxidation over a broad visible-light range, Adv. Funct. Mater. 24 (2014) 7754–7762.

[11] R.A. Sheldon, I.W.C.E. Arends, G.J. Ten Brink, A. Dijksman, Green, catalytic oxidations of alcohols, Accounts Chem Res 35 (2002) 774–781.

[12] J. Piera, J.E. Backvall, Catalytic oxidation of organic substrates by molecular oxygen and hydrogen peroxide by multistep electron transfer - A biomimetic approach, Angew. Chemie Int. Ed. English 47 (2008) 3506–3523.

[13] T.L. Lu, Z.T. Du, J.X. Liu, H. Ma, J. Xu, Aerobic oxidation of primary aliphatic alcohols over bismuth oxide supported platinum catalysts in water, Green Chem. 15 (2013) 2215–2221.

[14] J. Han, Y. Liu, R. Guo, Reactive template method to synthesize gold nanoparticles with controllable size and morphology supported on shells of polymer hollow microspheres and their application for aerobic alcohol oxidation in water, Adv. Funct. Mater. 19 (2009) 1112–1117.

[15] D.S. Mannel, M.S. Ahmed, T.W. Root, S.S. Stahl, Discovery of multicomponent heterogeneous catalysts via admixture screening: PdBiTe catalysts for aerobic oxidative esterification of primary alcohols, J. Am. Chem. Soc. 139 (2017) 1690–1698.

[16] C. Keresszegi, T. Mallat, J.D. Grunwaldt, A. Baiker, A simple discrimination of the promoter effect in alcohol oxidation and dehydrogenation over platinum and palladium, J. Catal. 225 (2004) 138–146.

[17] R.K. Bowman, A.D. Brown, J.H. Cobb, J.F. Eaddy, M.A. Hatcher, M.R. Leivers, J.F. Miller, M.B. Mitchell, D.E. Patterson, M.A. Toczko, S.P. Xie, Synthesis of HCV replicase inhibitors: base-catalyzed synthesis of protected alpha-hydrazino esters and selective aerobic oxidation with catalytic Pt/Bi/C for synthesis of Imidazole-4,5-dicarbaldehyde, J. Org. Chem. 78 (2013) 11680–11690.

[18] D.S. Mannel, J. King, Y. Preger, M.S. Ahmed, T.W. Root, S.S. Stahl, Mechanistic insights into aerobic oxidative methyl esterification of primary alcohols with heterogeneous PdBiTe catalystsy, ACS Catal. 8 (2018) 1038–1047.

[19] A. Gabrielsson, P.W.N.M. van Leeuwen, W. Kaim, Acidic iridium hydrides: implications for aerobic and Oppenauer oxidation of alcohols, Chem. Commun. (Camb.) (2006) 4926–4927.

[20] B. Jiang, Y. Feng, E.A. Ison, Mechanistic investigations of the iridium(III)-Catalyzed aerobic oxidation of primary and secondary alcohols, J. Am. Chem. Soc. 130 (2008) 14462–14464.

[21] K. Fujita, N. Tanino, R. Yamaguchi, Ligand-promoted dehydrogenation of alcohols catalyzed by Cp*Ir complexes. A new catalytic system for oxidant-free oxidation of alcohols, Org. Lett. 9 (2007) 109–111.

[22] A. Gunay, M.A. Mantell, K.D. Field, W.B. Wu, M. Chin, M.H. Emmert, Oxidation catalysis in air with Cp*Ir: influence of added ligands and reaction conditions on catalytic activity and stability, Catal. Sci. Technol. 5 (2015) 1198–1205.

[23] R. Kawahara, K. Fujita, R. Yamaguchi, Dehydrogenative oxidation of alcohols in aqueous media using water-soluble and reusable cp*Ir catalysts bearing a functional bipyridine ligand, J. Am. Chem. Soc. 134 (2012) 3643–3646.

[24] C. Hammond, M.T. Schumperli, S. Conrad, I. Hermans, Hydrogen transfer processes mediated by supported iridium oxide nanoparticles, Chemcatchem 5 (2013) 2983–2990.

[25] S. Abednatanzi, P.G. Derakhshandeh, A. Abbasi, P. Van der Voort, K. Leus, Direct synthesis of an iridium(III) bipyridine metal-organic framework as a heterogeneous catalyst for aerobic alcohol oxidation, Chemcatchem 8 (2016) 3672–3679.

[26] G.H. Gunasekar, K. Park, V. Ganesan, K. Lee, N.K. Kim, K.D. Jung, S. Yoon, A covalent triazine framework, functionalized with Ir/N-Heterocyclic carbene sites, for the efficient hydrogenation of CO2 to formate, Chem. Mater. 29 (2017) 6740–6748.

[27] C.E. Chan-Thaw, A. Villa, P. Katekomol, D.S. Su, A. Thomas, L. Prati, Covalent triazine framework as catalytic support for liquid phase reaction, Nano Lett. 10 (2010) 537–541.

[28] J. Artz, Covalent triazine-based FrameworksTailor-made catalysts and catalyst supports for molecular and nanoparticulate species, Chemcatchem 10 (2018) 1753–1771.

[29] P. Kuhn, A. Thomas, M. Antonietti, Toward tailorable porous organic polymer networks: a high-temperature dynamic polymerization scheme based on aromatic nitriles, Macromolecules 42 (2009) 319–326.

[30] R. Palkovits, M. Antonietti, P. Kuhn, A. Thomas, F. Schuth, Solid catalysts for the selective low-temperature oxidation of methane to methanol, Angew. Chemie Int. Ed. English 48 (2009) 6909–6912.

[31] K. Iwase, T. Yoshioka, S. Nakanishi, K. Hashimoto, K. Kamiya, Copper-modified covalent triazine frameworks as non-noble-Metal electrocatalysts for oxygen reduction, Angew. Chemie Int. Ed. English 54 (2015) 11068–11072.

[32] C.B. Lu, J. Yang, S. Wei, S. Bi, Y. Xia, M.X. Chen, Y. Hou, M. Qiu, C. Yuan, Y.Z. Su, F. Zhang, H.W. Liang, X.D. Zhuang, Atomic Ni anchored covalent triazine framework as high efficient electrocatalyst for carbon dioxide conversion, Adv. Funct. Mater. 29 (2019).

[33] J. Artz, S. Mallmann, R. Palkovits, Selective aerobic oxidation of HMF to 2,5-Diformylfuran on covalent triazine frameworks-supported Ru catalysts, Chemsuschem 8 (2015) 672–679.

[34] S. Rajendiran, P. Natarajan, S. Yoon, A covalent triazine framework-based heterogenized Al-Co bimetallic catalyst for the ring-expansion carbonylation of epoxide to beta-lactone, RSC Adv. 7 (2017) 4635–4638.

[35] S. Hug, M.E. Tauchert, S. Li, U.E. Pachmayr, B.V. Lotsch, A functional triazine framework based on N-heterocyclic building blocks, J. Mater. Chem. 22 (2012) 13956–13964.

[36] M.T. Youinou, R. Ziessel, Synthesis and Molecular-Structure of a New Family of Iridium(Iii) and Rhodium(Iii) Complexes - [Eta-5-Me5c5)Ir(Ll)X] + and [Eta-5-Me5c5)Rh(Ll)Cl] + - Ll = 2,2'-Bipyridine or 1,10-Phenanthroline - X = Cl or H - Single-Crystal Structures of [Eta-5-Me5c5)Ir(Bpy)Cl]Cl and [Eta-5-Me5c5)Rh (Phen)Cl]Clo4, J. Organomet. Chem. 363 (1989) 197–208.

[37] H. Watanabe, S. Asano, S. Fujita, H. Yoshida, M. Arai, Nitrogen-Doped, Metal-Free Activated Carbon Catalysts for Aerobic Oxidation of Alcohols, ACS Catal. 5 (2015) 2886–2894.

[38] Y.H. Cao, H. Yu, F. Peng, H.J. Wang, Selective allylic oxidation of cyclohexene catalyzed by nitrogen-doped carbon nanotubes, ACS Catal. 4 (2014) 1617–1625.

[39] N. Gupta, O. Khavryuchenko, A. Villa, D.S. Su, Metal-free oxidation of glycerol over nitrogen-containing carbon nanotubes, Chemsuschem 10 (2017) 3030–3034.

[40] J.L. Long, X.Q. Xie, J. Xu, Q. Gu, L.M. Chen, X.X. Wang, Nitrogen-doped graphene nanosheets as metal-free catalysts for aerobic selective oxidation of benzylic alcohols, ACS Catal. 2 (2012) 622–631.

[41] X.G. Duan, H.Q. Sun, Y.X. Wang, J. Kang, S.B. Wang, N-doping-Induced nonradical reaction on single-walled carbon nanotubes for catalytic phenol oxidation, ACS Catal. 5 (2015) 553–559.

[42] H. Yu, F. Peng, J. Tan, X.W. Hu, H.J. Wang, J.A. Yang, W.X. Zheng, Selective catalysis of the aerobic oxidation of cyclohexane in the liquid phase by carbon nanotubes, Angew. Chemie Int. Ed. English 50 (2011) 3978–3982.

[43] S. Navalon, A. Dhakshinamoorthy, M. Alvaro, M. Antonietti, H. Garcia, Active sites on graphene-based materials as metal-free catalysts, Chem. Soc. Rev. 46 (2017) 4501–4529.

[44] G. Tuci, M. Pilaski, H. Ba, A. Rossin, L. Luconi, S. Caporali, C. Pham-Huu, R. Palkovits, G. Giambastiani, Unraveling surface basicity and bulk morphology relationship on covalent triazine frameworks with unique catalytic and gas adsorption properties, Adv. Funct. Mater. 27 (2017).

[45] D.Y. Osadchii, A.I. Olivos-Suarez, A.V. Bavykina, J. Gascon, Revisiting nitrogen species in covalent triazine frameworks, Langmuir 33 (2017) 14278–14285.

[46] G.R. Buettner, Spin trapping - electron-spin-Resonance parameters of spin adducts, Free Radical Bio Med 3 (1987) 259–303.

[47] W. Huang, B.C. Ma, H. Lu, R. Li, L. Wang, K. Landfester, K.A.I. Zhang, Visible-light-Promoted selective oxidation of alcohols using a covalent triazine framework, ACS Catal. 7 (2017) 5438–5442.